Studies on Mixed Metal(II)–Iron(II) Chloride Systems. Part 2.[1] Mössbauer and *X*-Ray Powder Diffraction Data † for the Potassium and Rubidium $M'M''_xFe_{1-x}Cl_3\cdot 2H_2O$ (M' = K or Rb; M'' = Mn, Co, or Ni; x = 0.5) Systems

Bella Y. Enwiya and Jack Silver *
Department of Chemistry, University of Essex, Wivenhoe Park, Colchester CO4 3SQ, Essex
Ian E. G. Morrison
Department of Chemistry, Imperial College, London SW7 2AZ

The potassium and rubidium complexes $M'M''_xFe_{1-x}\cdot 2H_2O$ (M' = K or Rb; M'' = Mn, Co, or Ni; x = 0.5) have been studied by Mössbauer spectroscopy and *X*-ray powder diffraction. The first occurrence of an octahedral Fe^{II} environment containing four chlorides and two *cis* water molecules is reported for the Rb materials. The K materials contain octahedral Fe^{II} environments with *trans* water molecules. The ^{57}Fe Mössbauer data for these compounds are presented. The chemical shifts of both sets of materials are similar, but the quadrupole splitting data are different. The data for the Rb materials are explained in terms of changes in site symmetry and orbital occupancy. The changes are brought about by changes in bonding due to 'pressure' effects. The occurrence of *cis–trans* isomers in the mother-solutions is discussed.

In Mössbauer and *X*-ray powder diffraction studies[1] of $M_xFe_{1-x}Cl_2\cdot 4H_2O$ (M = Mn, Co, or Ni; x = 0—0.75) we found that the quadrupole splittings decreased significantly for the Fe–Co and Fe–Ni systems. These effects were explained in terms of changes in site symmetry resulting in an alteration of orbital occupancy from d_{xy} to d_{xz},d_{yz}. The changes in site symmetry were caused by changes in Fe–OH_2 bonding in the lattices 'squeezing' the Fe^{II} centres. The Fe–Mn system also gave results which appeared to be directly related to volume change but no evidence was found for pressure effects. These interesting changes were quite different to those we found in the perovskite $KFe_xM_{1-x}F_3$ (M = Mn, Co, Ni, and Zn; x = 0.5) compounds,[2,3] where small changes in quadrupole splitting were probably caused by interactions of the Fe^{II} ions with the other metal ions in the environment.

As such a range of quadrupole splittings was readily available by mixing other metal(II) and iron(II) chloride systems, we have extended these studies to other Fe^{II} chloride hydrate systems.

We report here the results of *X*-ray powder diffraction and Mössbauer spectroscopic studies of the $M'M''_xFe_{1-x}Cl_3\cdot 2H_2O$ (M' = K or Rb; M'' = Mn, Co, or Ni; x = 0.5) systems.

Experimental

The compounds were all prepared by the same method using the appropriate mol ratios for the required material; for example, for $KMn_{0.5}Fe_{0.5}Cl_3\cdot 2H_2O$ 2 : 1 : 1 mol ratios of KCl, $FeCl_2\cdot 4H_2O$, and $MnCl_2\cdot 4H_2O$ were used. A solution of $FeCl_2\cdot 4H_2O$ was boiled with a small amount of ascorbic acid (present as a reducing agent against Fe^{III}) and a solution containing the appropriate transition-metal chloride added. The resulting solution was heated to near dryness in an N_2 atmosphere. Analytical data for the $M'M''_{0.5}Fe_{0.5}Cl_3\cdot 2H_2O$ (M' = K or Rb; M'' = Mn, Fe, Co, or Ni) compounds appear in Table 1. Analyses were carried out in our laboratory. The compounds are sensitive to oxidation and were handled under an N_2 atmosphere. *X*-Ray powder diffraction data of the products were obtained using a Philips 11.64 cm powder camera and Cu-K_α radiation.

Table 1. Analytical data (%) * for the compounds $M'M''FeCl_3\cdot 2H_2O$ (M' = K or Rb; M'' = Mn, Fe, Co, or Ni)

Phase	Fe	M	Cl
$KFeCl_3\cdot 2H_2O$	21.5		41.0
	(23.55)		(44.8)
$KMn_{0.5}Fe_{0.5}Cl_3\cdot 2H_2O$	11.5	11.5	44.5
	(11.8)	(11.6)	(44.9)
$KCo_{0.5}Fe_{0.5}Cl_3\cdot 2H_2O$	11.2	11.8	43.9
	(11.7)	(12.35)	(44.55)
$KNi_{0.5}Fe_{0.5}Cl_3\cdot 2H_2O$	11.5	12.1	44.0
	(11.7)	(12.3)	(44.55)
$RbFeCl_3\cdot 2H_2O$	19.8		36.3
	(19.7)		(37.5)
$RbMn_{0.5}Fe_{0.5}Cl_3\cdot 2H_2O$	10.0	9.8	37.2
	(9.85)	(9.7)	(37.55)
$RbCo_{0.5}Fe_{0.5}Cl_3\cdot 2H_2O$	9.9	10.3	37.0
	(9.8)	(10.35)	(37.3)
$RbNi_{0.5}Fe_{0.5}Cl_3\cdot 2H_2O$	9.8	10.6	37.1
	(9.8)	(10.3)	(37.3)

* Calculated values in parentheses.

The analytical results (and Mössbauer data) show that $KFeCl_3\cdot 2H_2O$ was not prepared pure. The Fe^{II} analysis results tend to be slightly high due to the presence of a very small amount of ascorbic acid. However, the analyses for the compounds $KM''_{0.5}Fe_{0.5}Cl_3\cdot 2H_2O$ (M'' = Mn, Co, and Ni) are acceptable.

The preparation of mixed compounds of the general formula $K_2M''_{0.5}Fe_{0.5}Cl_4\cdot 2H_2O$ (M'' = Mn, Fe, Co, or Ni) were also attempted but all preparations resulted in mixtures of KCl and $KM''_{0.5}Fe_{0.5}Cl_3\cdot 2H_2O$. This is not surprising as Süss[4] reported that $K_2MnCl_4\cdot 2H_2O$ must be prepared above 28.2 °C (our method for mixed compounds required evaporation to dryness).

The Mössbauer apparatus has been described previously.[1] The source was 8 mCi ^{57}Co/Cu. The solid absorbers were finely powdered and sealed in a Perspex holder with Sellotape. The absorber thickness was *ca.* 0.02 g cm^{-2}. Velocity calibrations were carried out using thin 10 mg cm^{-2} high-purity iron foils. The spectra were analysed by a simple non-linear least-

† *Supplementary data available* (No. SUP 23549, 5 pp.): *X*-ray powder diffraction data.

Table 2. Unit-cell sizes for the potassium and rubidium salts calculated from *X*-ray powder diffraction data

Compound	*a*/Å	*b*/Å	*c*/Å	α/°	β/°	γ/°
$KMnCl_3·2H_2O$ [a]	6.49	6.91	9.91	96.8	114.1	112.6
$KFeCl_3·2H_2O$	6.32(1)	6.72(1)	9.71(1)	96.6	113.8	112.4
$KMn_{0.5}Fe_{0.5}Cl_3·2H_2O$	6.43(1)	6.82(1)	9.81(1)	96.7	113.8	112.5
$KCo_{0.5}Fe_{0.5}Cl_3·2H_2O$	6.28(1)	6.68(1)	9.69(1)	96.6	113.8	112.3
$KNi_{0.5}Fe_{0.5}Cl_3·2H_2O$	6.28(1)	6.68(1)	9.68(1)	96.4	113.6	112.2
α-$RbMnCl_3·2H_2O$ [b]	9.005	7.055	11.340			
$RbFeCl_3·2H_2O$ [c]	8.94(1)	6.96(1)	11.26(1)			
	8.876 [d]	6.872 [d]	11.181 [d]			
$RbMn_{0.5}Fe_{0.5}Cl_3·2H_2O$ [c]	8.97(1)	7.00(1)	11.30(1)			
$RbCo_{0.5}Fe_{0.5}Cl_3·2H_2O$ [c]	8.74(1)	6.69(1)	11.03(1)			
$RbNi_{0.5}Fe_{0.5}Cl_3·2H_2O$ [c]	8.64(1)	6.58(1)	10.95(1)			

[a] Data from ref. 5. [b] Data from ref. 6. [c] Orthorhombic. [d] Data from ref. 21.

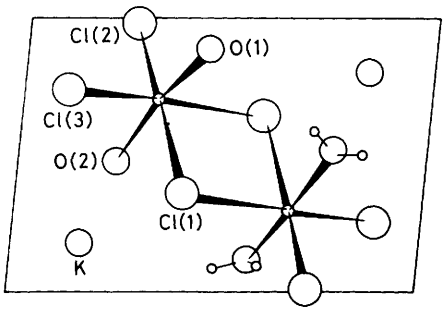

Figure 1. A projection of $KMnCl_3·2H_2O$ on (100)

squares fitting program; all isomer shifts are referred to natural iron.

Results and Discussion

The $KM''_{0.5}Fe_{0.5}Cl_3·2H_2O$ (M'' = Mn, Fe, Co, *or* Ni) *System.*—The *X*-ray powder diffraction data (see SUP No. 23549 and Table 2) show that the compounds $KM''_{0.5}Fe_{0.5}Cl_3·2H_2O$ (M'' = Mn, Fe, Co, or Ni) are isostructural with $KMnCl_3·2H_2O$.[5]

Crystal structure of $KMnCl_3·2H_2O$. This compound crystallizes in the triclinic space group *P*1, with two formula units per unit cell. The manganese atom is octahedrally co-ordinated to four chlorine atoms and two water molecules. The water molecules occupy *trans* positions (Figure 1). The octahedra are joined in pairs by sharing edges, forming discrete groups of $[Mn_2Cl_6]^{2-}·4H_2O$ ions. The structure can be described as a layer structure (the Mn atoms lie between these layers), where each layer, A, consists of chains of chlorine atoms only, alternating with chains containing the K and the O atoms [Figure 2(*a*)]. In $KMnCl_3·2H_2O$ [Figure 2(*b*)] the layers are parallel to (100), and the chains in all the layers are parallel to [011] so that the resulting overall sequence is -A-Mn-A-A-Mn-A.[6]

The major bond lengths found in the $KMnCl_3·2H_2O$ structure are given in Table 3. The Mn–OH_2 bond lengths are smaller than the Mn–Cl(1), Mn–Cl(2), and Mn–Cl(3) bond lengths, and the Mn–Cl(2) and Mn–Cl(3) bonds are slightly shorter than the Mn–Cl(1) bridging bonds. There is no indication of direct Mn–Mn interaction.

The potassium derivatives reported in this work show a range of change in cell dimensions of up to the order of 0.2 Å in each dimension from $KMnCl_3·2H_2O$. There is little alteration in the Mössbauer parameters for this range (see later) showing that the Fe^{II} electronic environments are largely

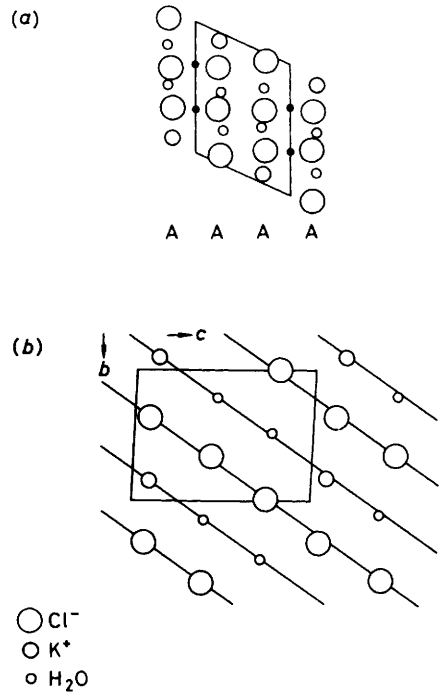

Figure 2. (*a*) Layer structure of $KMnCl_3·2H_2O$ seen in the direction of the *c* axis. (*b*) The A layer of $KMnCl_3·2H_2O$

unchanged. This can only be explained if the discrete $[M''FeCl_6]^{2-}·4H_2O$ (M'' = Mn, Fe, Co, or Ni) ions are not squeezed; the only other remaining ions that can yield in the structure are the K^+ ions. It is these K^+ ions that must slip closer to the $[M''FeCl_6]^{2-}·4H_2O$ ions to accommodate the lattice parameter changes.

The suggested hydrogen bonds in $KMnCl_3·2H_2O$ [5] between the $[Mn_2Cl_6]^{2-}·4H_2O$ ions are important in the mixed K materials. They must aid in the packing of the lattice, and change length to accommodate the changes in lattice parameters. Neither the change in proximity of the K^+ ions nor the change in H-bond length is obviously manifest on the electronic environment of the Fe^{II} ions.

Mössbauer data for the potassium system. The Mössbauer data (Table 4) are diagnostic of high-spin Fe^{II}.

In the high-spin Fe^{II} ion, the free-ion configuration ^5D-(t_{2g}^4, e_g^2) signifies a single 3*d* electron outside the spherical half-filled shell. In a ligand field of cubic symmetry with a regular octahedral ion environment the t_{2g} levels remain degenerate (as do the e_g) and there is no finite electric field

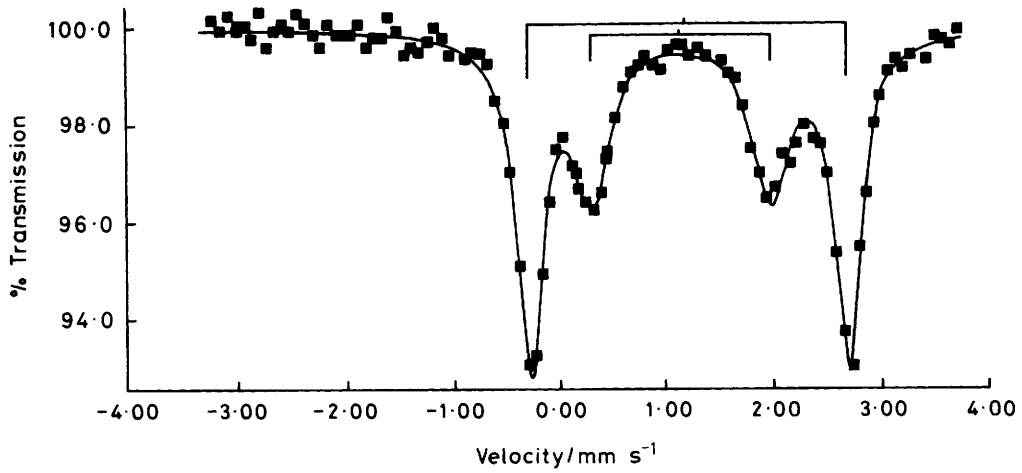

Figure 3. Mössbauer spectrum for $KFeCl_3 \cdot 2H_2O$ at 298 K

Table 3. Bond lengths (Å) for $KMnCl_3 \cdot 2H_2O$

(*a*) Within octahedra		(*b*) Between neighbouring octahedra	
Mn–Cl(1)	2.594(3), 2.570(5)	Mn · · · Mn	3.845(3)
Mn–Cl(2)	2.490(3)	Cl(1) · · · O(1)	3.179(14), 3.551(13)
Mn–Cl(3)	2.482(5)	Cl(2) · · · O(1)	3.223(11)
Mn–O(1)	2.182(12)	Cl(2) · · · O(2)	3.510(13), 3.140(8)
Mn–O(2)	2.187(11)	Cl(3) · · · O(2)	3.274(13)
(*c*) From the potassium atom			
K · · · Cl(1)	3.128(5), 3.587(4)	K · · · Cl(3)	3.606(7), 3.349(6), 3.121(4)
K · · · Cl(2)	3.241(7), 3.277(7), 4.855(6)	K · · · O(2)	3.164(10), 4.294(11), 4.469(13)
K · · · O(1)	3.316(12)		

Table 4. Iron-57 Mössbauer parameters for the high-spin iron(II) chlorides

Compound	*T*/K	δ/mm s^{-1}	Δ/mm s^{-1}	Γ/mm s^{-1}
$KFeCl_3 \cdot 2H_2O$	298	1.17(1)	1.65(1)	0.19(1)
	80	1.31(1)	2.57(5)	0.32(3)
$KMn_{0.5}Fe_{0.5}Cl_3 \cdot 2H_2O$	298	1.16(1)	1.80(1)	0.13(1)
	180	1.23(1)	2.21(1)	0.13(1)
	80	1.28(1)	2.47(1)	0.14(1)
$KCo_{0.5}Fe_{0.5}Cl_3 \cdot 2H_2O$	298	1.14(1)	1.80(1)	0.15(1)
	180	1.23(1)	2.28(1)	0.15(1)
	80	1.28(1)	2.50(1)	1.16(1)
$KNi_{0.5}Fe_{0.5}Cl_3 \cdot 2H_2O$	298	1.16(1)	1.78(1)	0.15(1)
	180	1.23(1)	2.24(1)	0.14(1)
	80	1.28(1)	2.50(1)	0.15(1)
$KFeCl_3$ [a]	298	1.10(1)	2.37(1)	0.32(1)
$KFeCl_3 \cdot 2H_2O$ [b]	298	1.22(1)	2.33(5)	0.21(8)
$FeCl_2 \cdot 2H_2O$ [c]	298	1.03	2.70	
	80	1.08	2.50	
$RbFeCl_3 \cdot 2H_2O$	298	1.16(2)	1.41(2)	0.12(1)
	80	1.28(2)	1.49(2)	0.13(2)
$RbMn_{0.5}Fe_{0.5}Cl_3 \cdot 2H_2O$	298	1.160(2)	1.386(4)	0.122(4)
	180	1.238(1)	1.435(3)	0.129(2)
	80	1.289(2)	1.461(3)	0.133(3)
$RbCo_{0.5}Fe_{0.5}Cl_3 \cdot 2H_2O$	298	1.165(3)	1.534(6)	0.121(5)
	180	1.232(2)	1.809(3)	0.133(3)
	80	1.284(1)	2.055(3)	0.133(2)
$RbNi_{0.5}Fe_{0.5}Cl_3 \cdot 2H_2O$	298	1.173(3)	1.541(5)	0.118(5)
	180	1.232(2)	1.783(3)	0.140(3)
	80	1.283(2)	2.000(4)	0.148(3)

[a] Data from ref. 7. [b] After dehydration. [c] Data from ref. 11.

gradient (e.f.g.). However, if the symmetry is lowered to trigonal or tetragonal, further degeneracy is removed. The sixth electron is in the appropriate lowest lying unfilled state, and now generates an e.f.g. at the iron nucleus.

The quadrupole splitting originates not from asymmetric covalency with the ligands, but from the sensitivity of the orbital state from an essentially non-bonding electron to the geometrical environment.

The compound $KFeCl_3 \cdot 2H_2O$ was never prepared pure (see Experimental section). This was confirmed by Mössbauer spectroscopy which always showed the presence of $FeCl_2 \cdot 4H_2O$ (Figure 3). However, the parameters of a second iron environment which was that of $KFeCl_3 \cdot 2H_2O$ are also present.

When the material from this preparation was dehydrated the resulting product gave Mössbauer parameters of δ 1.22(1) and Δ 2.33(5) mm s^{-1}; the quadrupole splitting value is similar to the literature value [7] for $KFeCl_3$ of 2.37(1) mm s^{-1} although the value for the isomer shift is 1.10(1) mm s^{-1}.

Mössbauer spectra for $KM''_{0.5}Fe_{0.5}Cl_3 \cdot 2H_2O$ (M'' = Mn, Co, or Ni) show the presence of only one Fe^{II} environment. The Mössbauer parameters for this site are all very similar (Table 4) and not too different from the second site in the compound $KFeCl_3 \cdot 2H_2O$.

The quadrupole splitting differences at a given temperature in these materials are very small suggesting that the Fe^{II} environments are hardly changed despite the presence of another transition metal. Therefore the changes in cell size caused by the introduction of another transition metal mainly affect the potassium layers and the hydrogen bonds. They do so in such a way that there are no extra pressure effects on the Fe^{II} environment. The isomer shifts for these materials are similar to that of $KFeCl_3 \cdot 2H_2O$ and indicate that the amounts of *s*-electron density (contribution) in the bond are approximately equal. Also the *p*- and *d*-electron shielding must be similar and again *p*- and *d*-electron contribution to the bonding must be similar.

Drickamer and co-workers [8] predicted a decrease in the isomer shift with increasing pressure corresponding to an increase of *s*-electron density at the iron nucleus, which is associated with changes in $3d$–$3s$ shielding. The slight

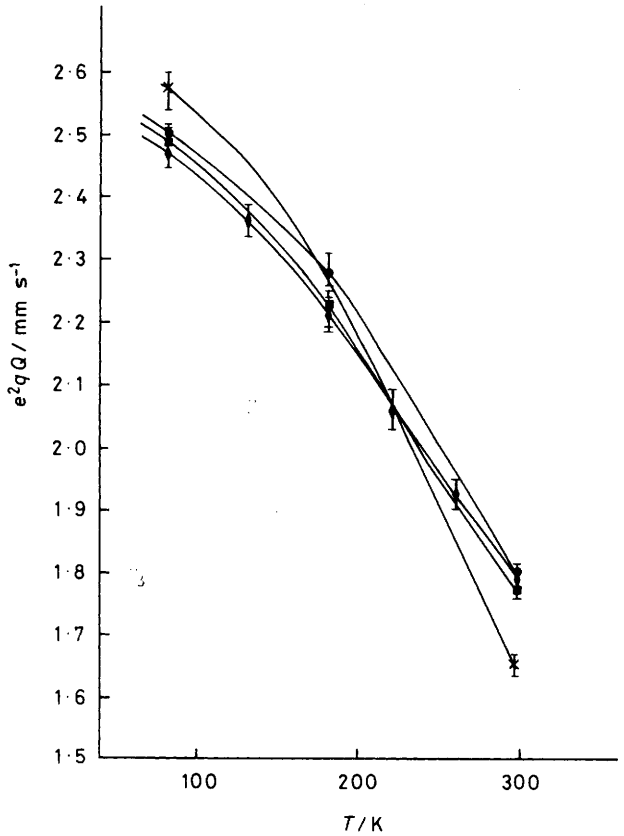

Figure 4. Temperature dependence of the quadrupole splitting of the $KM''_{0.5}Fe_{0.5}Cl_3 \cdot 2H_2O$ [M'' = Fe (×), Mn (♦), Co (●), or Ni (■)] materials

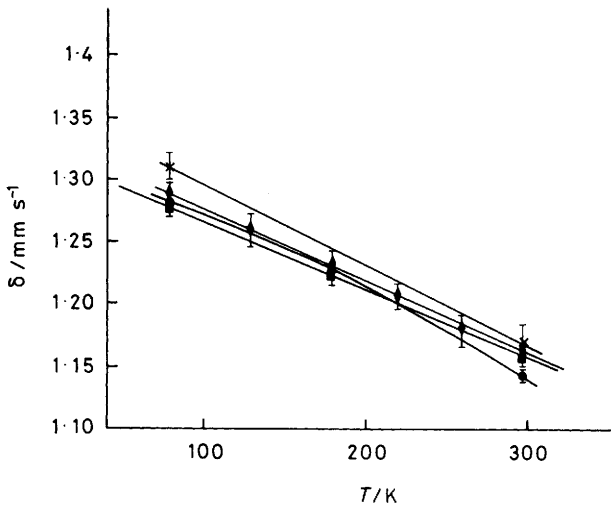

Figure 5. Chemical isomer shift *versus* temperature of the $KM''_{0.5}Fe_{0.5}Cl_3 \cdot 2H_2O$ [M'' = Fe (×), Mn (♦), Co (●), or Ni (■)] materials

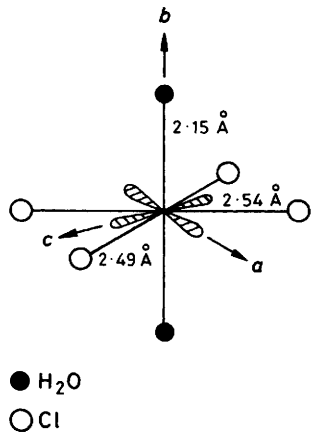

Figure 6. Local environment of $FeCl_2 \cdot 2H_2O$; all Cl^- ions are bridging (*a*, *b*, and *c* are the crystallographic axes)

change in the isomer shift relative to $KFeCl_3 \cdot 2H_2O$ for these compounds is in keeping with their work, but we did not observe an increase in the quadrupole splitting at 80 K.

The $KM''_{0.5}Fe_{0.5}Cl_3 \cdot 2H_2O$ (M'' = Mn, Fe, Co, or Ni) system shows significant temperature dependence of the quadrupole splitting and isomer shift; these changes are gradual and rule out a phase change (Figures 4 and 5).

The structure of these compounds is discussed above (Figure 1). The Fe^{II} ions lie in distorted octahedral environments with four Cl atoms (two of which are bridging) in a plane and the two water molecules are in *trans* positions. The Fe^{II} environment can be described as close to tetragonal. The sixth Fe^{II} electron occupies the lowest lying unfilled state. A ligand field of axial symmetry (*i.e.* a tetragonal distortion of the octahedron) will split the t_{2g} state into a lower d_{xy} single level and an upper d_{xz},d_{yz} state.[9]

In these compounds the d_{xy} is the ground state and the sixth electron occupies this state, generating a quadrupole splitting in proportion to $V_{zz}/e = q = \frac{4}{7} \langle r^{-3} \rangle (1 - R)/(4\pi\varepsilon_0)$, where R = 'atomic' Sternheimer factor and ε_0 = permittivity of a vacuum.[9] This is a singlet ground state for which e^2qQ (quadrupole splitting) is positive.

At a very high temperature all the levels of the t_{2g} multiplet would be equally populated by thermal excitation and the e.f.g. would be zero. The temperature dependence of the quadrupole splitting in the $KM''_{0.5}Fe_{0.5}Cl_3 \cdot 2H_2O$ system is primarily due to the Boltzman population of the d^6 manifolds. A partial degree of thermal excitation will cause a partial cancellation of the e.f.g., so that the quadrupole splitting should decrease with increasing temperature. A full mathematical treatment of the temperature dependence is given by Ingalls.[10] The limiting value of the quadrupole splitting (*ca.* 2.5 mm s^{-1} in this case) at lower temperatures relates to the orbital state of the lowest lying levels and the significant decrease with increasing temperature relates to the population of many low lying excited states.

The compounds $KM''_{0.5}Fe_{0.5}Cl_3 \cdot 2H_2O$ (M'' = Mn, Fe, Co, or Ni) show Mössbauer parameters similar to those of $FeCl_2 \cdot 2H_2O$ [11,12] at 80 K. In $FeCl_2 \cdot 2H_2O$ [11] the local environment about each iron has a monoclinic symmetry and consists of four chlorine ions arranged in a slightly distorted square planar configuration and two water molecules, one above and one below the iron–chlorine plane (Figure 6). Each chlorine ion is shared by two Fe^{II} ions. The resulting Fe^{II} environment in $FeCl_2 \cdot 2H_2O$ is a distorted octahedron.

For $FeCl_2 \cdot 2H_2O$ the octahedral part of the crystal field partially lifts the five-fold orbital degeneracy to leave a doublet (e_g state) considerably higher in energy than the triplet t_{2g}. The non-cubic components of the crystal field remove the remainder of the degeneracy of the three t_{2g} states. The total e.f.g. at the nucleus includes a direct contribution from the other ions in the lattice as well as the contribution from the electron orbitals of the Fe^{II} ion.

The Mössbauer data at room and liquid nitrogen tempera-

ture for $FeCl_2 \cdot 2H_2O$ are given in Table 4. The quadrupole splitting temperature dependence in $FeCl_2 \cdot 2H_2O$ is consistent with a ground state which is predominantly a d_{xy}. However, $FeCl_2 \cdot 2H_2O$ [11-18] shows a small temperature dependence of the quadrupole splitting and presumably signifies that in this compound the excited states are separated by greater energies from the ground state.

It is worth noting that the $KM''_{0.5}Fe_{0.5}Cl_3 \cdot 2H_2O$ (M'' = Mn, Fe, Co, or Ni) compounds never show the same isomer shift and quadrupole splitting exhibited by $FeCl_2 \cdot 2H_2O$. This is expected and reflects the fact that all the Cl^- ions are bridging in $FeCl_2 \cdot 2H_2O$.[19] However, it is apparent that the structural similarity of $FeCl_2 \cdot 2H_2O$ to the compounds discussed here is the factor which causes the similar quadrupole splitting observed at 80 K.

The quadrupole splitting may also be affected by the temperature dependence of the ligand-field splittings and the lattice term caused as a direct result of thermal expansion. Only the lattice cell constant is expected to change gradually with temperature, so the decrease in quadrupole splitting could also obviously be related to increased cell size.[9]

The gradual decrease of the quadrupole splitting of $KM''_{0.5}Fe_{0.5}Cl_3 \cdot 2H_2O$ could also be caused either by less distortion of the ligand electronic field as the lattice expands, or changes in the symmetry of the *d*-electron distribution imposed by the Fe^{II} ion itself, as found for $[Fe(H_2O)_6]^{2+}$ [20] and $[FeCl_2(H_2O)_4]$.[1]

The decrease in isomer shift with increasing temperature corresponds to an increase in *s*-electron density at the nucleus (which is expected due to lattice expansion), although the major temperature contribution to the isomer shift is the relativistic second-order Döppler shift.

The only other important question remaining is whether the dimeric units in these mixed materials (Figure 1) contain one Fe^{II} ion and one other M^{II} ion (M = Mn, Fe, Co, or Ni) or does each dimeric unit contain two Fe^{II} ions or the same two M^{II} ions?

It might be expected that for the former case the Mössbauer parameters would be different for each different M^{II} ion due to the changes in the Cl^- bridge bonding and also due to the different number of *d* electrons and 3*d* configuration of the other M^{II} ion. No such changes in the Mössbauer parameters are observed. Moreover, in the crystal structure of $KMnCl_3 \cdot 2H_2O$ [5] the Mn · · · Mn distance is 3.84 Å within the dimeric unit but is much greater between units (over 5.5 Å). The former distance is of the order of the metal–metal distance in $KM''_{0.5}Fe_{0.5}F_3$ (M'' = Mn, Co, Ni, or Zn) [3] compounds where small changes in quadrupole splitting were caused by interactions with other transition metals in the perovskite lattice.[4] The latter distance, however, would be too large for such interactions to affect the Fe^{II} electronic environments. Therefore it appears that in these mixed compounds the dimeric units contain the same transition metal, and it is the inclusion of different units in the packing which satisfies the overall formulation. The different units must be orderly (not randomly) packed or broad lines would be observed in the *X*-ray diffraction powder data.

The $RbM''_{0.5}Fe_{0.5}Cl_3 \cdot 2H_2O$ (M'' = Mn, Fe, Co, *or* Ni) *System.*—The *X*-ray powder diffraction data (see SUP No. 23549) shows that the compounds $RbM''_{0.5}Fe_{0.5}Cl_3 \cdot 2H_2O$ (M'' = Mn, Fe, Co, or Ni) are isostructural with α-$RbMnCl_3 \cdot 2H_2O$.[6]

Crystal structure of α-$RbMnCl_3 \cdot 2H_2O$.[6] This compound crystallizes in the orthorhombic space group *Pcca*, with four formula units per unit cell. The manganese atom is octahedrally co-ordinated to four chlorine atoms and two water molecules. The water molecules occupy *cis* positions and the octahedra form infinite chains by corner sharing at a chlorine atom (Figure 7). Neighbouring chains have weak coupling in the *c* direction by hydrogen bonding, and are separated in the *b* direction by planes of cations (Rb^+).

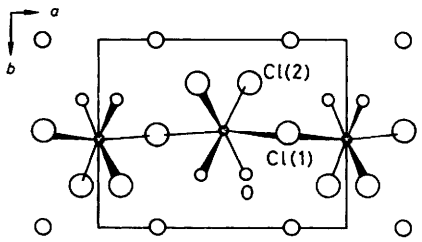

Figure 7. Projection of half the unit cell of α-$RbMnCl_3 \cdot 2H_2O$ on (001)

The phase α-$RbMnCl_3 \cdot 2H_2O$ [6] is said to be the stable form at 0 °C whereas β-$RbMnCl_3 \cdot 2H_2O$ (which is isostructural with the $KM''_{0.5}Fe_{0.5}Cl_3 \cdot 2H_2O$ series) is the stable form at 25 °C. In this work all the rubidium materials prepared containing Fe^{II} possessed the former structure. The complex $RbFeCl_3 \cdot 2H_2O$ has been prepared previously [15] at 37 °C, and its magnetic properties at very low temperatures 0—25 K have been extensively studied.[21-23] The compounds $RbMCl_3 \cdot 2H_2O$ (M = Co or Fe) have been found to be isostructural with α-$RbMnCl_3 \cdot 2H_2O$.[23,24]

For the $RbM''_{0.5}Fe_{0.5}Cl_3 \cdot 2H_2O$ (M = Mn, Co, or Ni) materials sharp lines in the *X*-ray powder diffraction data show that they are distinct (discrete) phases and not mixtures of the parent compounds. This means that the iron and other transition metals must be on random positions in the chains. Their cell sizes are smaller than those of the parent compound α-$RbMnCl_3 \cdot 2H_2O$ (Table 3).

The major bond lengths calculated from the cell dimensions and assuming the atom co-ordinates are those of α-$RbMnCl_3 \cdot 2H_2O$ [6] are given in Table 5. The M–OH_2 and M–Cl(2) bond lengths are smaller than the M–Cl(1) bridging distances. An examination of the differences in cell size and the differences in bond lengths (caused by replacement of one transition metal with another) indicates that the greater changes are in the *b* and *c* directions, affecting the M–OH_2 and M–Cl(2) bonds more than the bridging M–Cl(1) bonds that lie along the chain in the *a* direction (Figure 7). Therefore squeezing forces are more likely to affect the *bc* plane. The squeezing in the *c* direction also affects the hydrogen bonding between the octahedra and must confine the Rb ions.

The hydrogen bonding between the chains is important in the packing (and/or squeezing) as suggested in the parent α-$RbMnCl_3 \cdot 2H_2O$.[6] The hydrogen bonds change as one transition metal is substituted for another (Table 5). They lie in the *bc* plane principally in the direction shown below, where the arrows indicate the direction of H bonding.

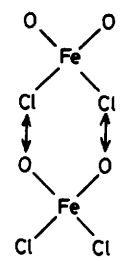

As this direction shows most evidence of squeezing, then as a result the Fe^{II} ion will experience changes in crystal-field splitting.

Table 5. Comparison of major bond lengths found in $RbM''_{0.5}Fe_{0.5}Cl_3 \cdot 2H_2O$ (M'' = Mn, Fe, Co, or Ni) with the parent α-$RbMnCl_3 \cdot 2H_2O$

Within octahedra	α-$RbMnCl_3 \cdot 2H_2O$	$RbFeCl_3 \cdot 2H_2O$	$RbMn_{0.5}Fe_{0.5}Cl_3 \cdot 2H_2O$	$RbCo_{0.5}Fe_{0.5}Cl_3 \cdot 2H_2O$	$RbNi_{0.5}Fe_{0.5}Cl_3 \cdot 2H_2O$
M–Cl(1)	2.549	2.53	2.54	2.48	2.45
M–Cl(2)	2.531	2.50	2.52	2.43	2.40
M–O	2.177	2.15	2.16	2.09	2.06
Between neighbouring octahedra					
Cl(1) · · · Cl(2)	3.892	3.73	3.74	3.76	3.72
Cl(1) · · · O	3.730	3.70	3.71	3.62	3.58
Cl(2) · · · O	3.697	3.33	3.35	3.20	3.15
Cl(2) · · · O	3.176	3.16	3.17	3.08	3.05
Cl(2) · · · O	3.186	3.17	3.18	3.10	3.07

In $RbM''_{0.5}Fe_{0.5}Cl_3 \cdot 2H_2O$ (M'' = Co or Ni), the Co^{II} and Ni^{II} ions are both smaller than Fe^{II} and thus the Fe^{II} is squeezed relative to its normal environment. As the greatest squeezing is in the *bc* plane this will split any remaining degeneracy in the t_{2g} levels.

For $RbMn_{0.5}Fe_{0.5}Cl_3 \cdot 2H_2O$ the Mn^{II} ions are larger than the Fe^{II}, and the unit-cell size is larger than that of $RbFeCl_3 \cdot 2H_2O$. Therefore the Fe^{II} ions are in larger spaces (holes) than usual and the result should be a more symmetrical Fe^{II} electronic environment as the Fe^{II} has room to move. This should result in a smaller crystal-field splitting of the *d* orbitals.

Mössbauer data for the rubidium system. The Mössbauer data for the Rb materials appear in Table 4 (Figures 8 and 9). Mössbauer data for $RbFeCl_3 \cdot 2H_2O$ and those of $RbM''_{0.5}Fe_{0.5}Cl_3 \cdot 2H_2O$ (M'' = Mn) are similar as might be expected for isostructural compounds. However, the following differences are observed, for the compounds with M'' = Co and Ni. (*a*) The quadrupole splittings for $RbM''_{0.5}Fe_{0.5}Cl_3 \cdot 2H_2O$ (M'' = Fe and Mn) are smaller than those for the Co- and Ni-containing compounds at all temperatures. (*b*) The quadrupole splittings of the Co and Ni derivatives show a significant temperature dependence (Figure 9). (*c*) The Ni derivative shows a larger isomer shift than the Co compound at room temperature, but not at the other temperatures. Plotting the isomer shifts and the quadrupole splittings against temperature for these materials gives nearly straight lines (Figures 8 and 9).

Mössbauer data for $RbFeCl_3 \cdot 2H_2O$ have recently been reported by Le Fever *et al.*[25,26] These authors show that the temperature dependence of their data indicates an orbital doublet ground state for iron(II).

Our data for $RbFeCl_3 \cdot 2H_2O$ agree well with the previous report.[25] The quadrupole splitting data for $RbMn_{0.5}Fe_{0.5}Cl_3 \cdot 2H_2O$ are similar to those of the parent $RbFeCl_3 \cdot 2H_2O$, but they are smaller. This Mn derivative has a larger cell size than the parent $RbFeCl_3 \cdot 2H_2O$ compound. Here, the Fe^{II} ions obviously sit in larger holes and thus are not squeezed; therefore they can find more symmetrical environments. It must obviously be this difference in cell size that causes the different quadrupole splitting behaviour.

The isomer shifts for the compounds $RbM''_{0.5}Fe_{0.5}Cl_3 \cdot 2H_2O$ (M'' = Fe, Mn, Co, and Ni) at 298 and 80 K are very similar. These Mössbauer data show that the Fe^{II} environments have similar *p*- and *d*-electron participation in the bonding of these materials.

The quadrupole splitting behaviour for the compounds $RbM''_{0.5}Fe_{0.5}Cl_3 \cdot 2H_2O$ (M'' = Co and Ni) is very similar suggesting that the iron electronic environments are very similar indeed. This, taken together with the isomer shift against temperature plot (Figure 8), gives no indication of a low-temperature phase change.

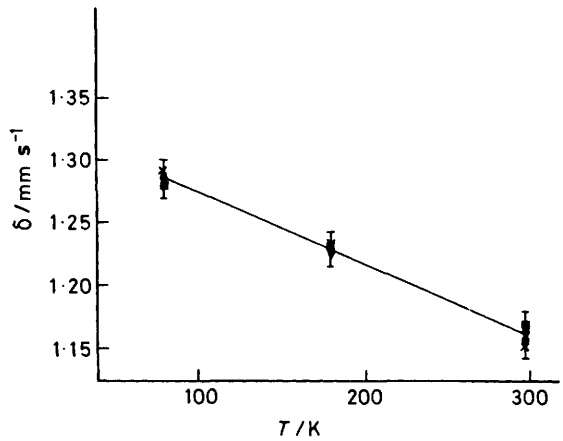

Figure 8. Chemical isomer shift *versus* temperature of the compounds $RbM''_{0.5}Fe_{0.5}Cl_3 \cdot 2H_2O$ [M'' = Fe (×), Mn (♦), Co (●), or Ni (■)]

The quadrupole splittings of both the Co^{II}- and Ni^{II}-substituted compounds are larger than the parent, showing that the crystal-field splitting is different, presumably caused by the squeezing effect of the substituted smaller transition metal.

The introduction of another transition metal in the lattice may cause changes in the symmetry of the Fe^{II} electronic environment and change the orbital occupancy. Also slight differences in the covalent contribution to the bonding, caused by the squeezing of the octahedra, may change the *d*-electron distribution.

In the Ni^{II}-substituted compound the quadrupole splitting is slightly smaller than the Co^{II}-substituted compound. This is expected as it is the smallest transition metal, and will cause more squeezing to Fe^{II} octahedra resulting in a greater change in electronic environment around Fe^{II} nuclei.

In $RbCo_{0.5}Fe_{0.5}Cl_3 \cdot 2H_2O$ and $RbNi_{0.5}Fe_{0.5}Cl_3 \cdot 2H_2O$ the cell sizes are smaller than that of $RbFeCl_3 \cdot 2H_2O$. These cell-size changes squeeze the M–Cl(2) and M–OH bonds in the lattices, as seen by changes in the quadrupole splitting. From this larger quadrupole splitting value it is likely that the orbital ground state is not the same as that for $RbFeCl_3 \cdot 2H_2O$. A singlet d_{xy} ground state would be expected to cause a larger splitting. Here the presence of Co and Ni in the lattices has caused a reversal of the tetragonal field so that the d_{xy} level is now the ground state. If the energy gap to the excited levels in this state was not large then the observed temperature dependence can be explained.

A complicating factor in the Rb compounds is the effect of

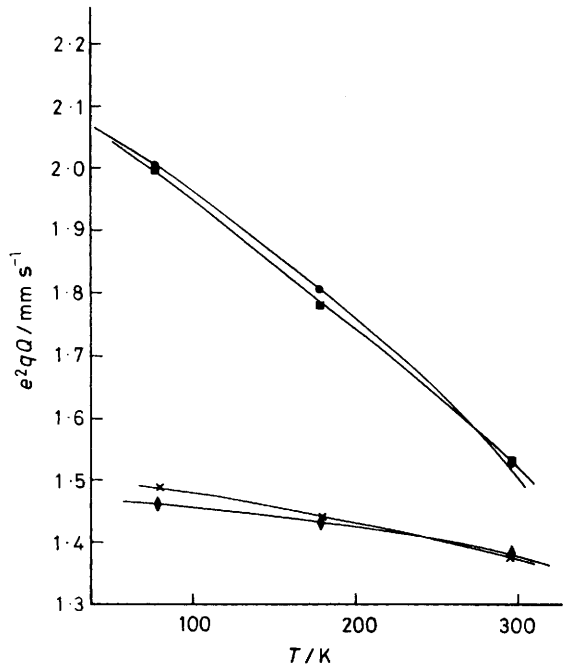

Figure 9. Temperature dependence of the quadrupole splitting of the compounds $RbM''_{0.5}Fe_{0.5}Cl_3 \cdot 2H_2O$ [M'' = Fe (×), Mn (♦), Co (●), or Ni (■)]

the different numbers of unpaired 3*d* electrons which the other transition metals pass on to the Fe^{II} electronic environments. It may well be that the Fe^{II} ions are being affected by these other ions as found in the $KM''_{0.5}Fe_{0.5}F_3$ compounds.[2] Indeed, the metal–metal distances in the chain (4.06—4.14 Å) are not much greater than those found in $KM''_{0.5}Fe_{0.5}F_3$ (M'' = Co, Ni, Mn, or Fe).

In fact, these long-range effects would be very small as the entire lattice effect appears to be usually less than 10% of the total e.f.g., as this lattice effect is the contribution to the e.f.g. tensor from the charges external to the central atom.[9]

Ingalls [10] considered the lattice contribution to be of opposite sign to that of the 3*d*-orbital contribution. It is essentially electrostatic in nature and will fall inversely proportional to r^2 (according to Coulomb's law): $F \propto 1/r^2$. The charges in the first co-ordination sphere will dominate this term, especially in non-cubic environments such as these chain structures.

The occurrence of *cis–trans* isomerism in kinetically labile co-ordination compounds is not common. The first established example of *cis–trans* isomerism in such materials was α- and β-$RbMnCl_3 \cdot 2H_2O$.[6] As yet in the Fe^{II}-containing materials we have not been able to isolate the β-phase with rubidium. However, this Fe^{II} *cis* water environment must have been present in the original solutions and the presence of a large cation such as rubidium was necessary to stabilize it in the solid form.

References

1 Part 1, B. Y. Enwiya, J. Silver, and I. E. G. Morrison, *J. Chem. Soc., Dalton Trans.*, 1982, 2231.
2 J. Silver and J. D. Donaldson, *Inorg. Nucl. Chem. Lett.*, 1976, **12**, 795.
3 J. Silver, *J. Fluorine Chem.*, 1976, **8**, 527.
4 J. Süss, *Z. Kristallogr. Mineral.*, 1912, **51**, 248.
5 S. J. Jenson, *Acta Chem. Scand.*, 1968, **22**, 641.
6 S. J. Jenson, *Acta Chem. Scand.*, 1967, **21**, 889.
7 D. H. Leech and D. J. Machin, *J. Inorg. Nucl. Chem.*, 1975, **37**, 2279.
8 A. R. Champion, R. W. Vaughan, and H. G. Drickamer, *J. Chem. Phys.*, 1961, **6**, 89.
9 T. C. Gibb, 'Principles of Mössbauer Spectroscopy,' Chapman and Hall, London and New York, 1976.
10 R. Ingalls, *Phys. Rev.*, 1964, **133**, A787.
11 S. Chandra and G. R. Hoy, *Phys. Lett.*, 1966, **22**, 254.
12 C. E. Johnson, *Proc. Phys. Soc.*, 1966, **88**, 943.
13 A. J. Nozik and M. Kaplan, *Phys. Rev.*, 1967, **159**, 273.
14 L. Kandel, M. A. Weber, R. B. Frankel, and C. R. Abeledo, *Phys. Lett. A.*, 1974, **46**, 369.
15 Y-Hazony, R. C. Axtmann, and J. W. Hurley, *J. Chem. Phys. Lett.*, 1968, **2**, 440.
16 I. Deszi, P. J. Ouseph, and P. M. Thomas, *Chem. Phys. Lett.*, 1971, **9**, 390.
17 B. Brunet, *J. Chem. Phys.*, 1974, **61**, 2360.
18 K. Burger, *Kem. Kozl.*, 1969, **32**, 69.
19 B. Morosin and E. J. G. Raeber, *J. Chem. Phys.*, 1965, **42**, 898.
20 D. L. Nagy, J. Balogh, I. Dezsi, G. Ritter, H. Spiering, and H. Vogel, *J. Phys. (Paris)*, 1980, **41**, C1-283.
21 Q. A. G. van Vlimmeren and W. J. M. de Jonge, *Phys. Rev. Sect. B*, 1979, **19**, 1503.
22 Q. A. G. van Vlimmeren, W. J. M. de Jonge, and M. S. J. Schuilwerve, *Ann. Israel Phys. Soc.*, 1978, **2**, 606.
23 K. Kopinga, Q. A. G. van Vlimmeren, A. L. Bongaarts, and W. J. M. de Jonge, *Physica*, 1977, **86–88B**, 671.
24 K. Koplinga, *Phys. Rev. Sect. B*, 1977, **16**, 427.
25 H. Th. Le Fever, R. C. Thiel, W. J. Huiskamp, and W. J. M. de Jonge, *Physica*, 1981, **111B**, 190.
26 H. Th. Le Fever, R. C. Thiel, W. J. Huiskamp, W. J. M. de Jonge, and A. M. Van der Kraan, *Physica*, 1981, **111B**, 209.

Received 9th August 1982; *Paper* 2/1387